1-1-2000

Dolomitization and Dolomite Neomorphism: Trenton and Black River Limestones (Middle Ordovician) Northern Indiana, U.S.A.

M. I N Chan

Jay M. Gregg
Missouri University of Science and Technology

Kevin L. Shelton

DOLOMITIZATION AND DOLOMITE NEOMORPHISM: TRENTON AND BLACK RIVER LIMESTONES (MIDDLE ORDOVICIAN) NORTHERN INDIANA, U.S.A.

CHAN MIN YOO[1]*, JAY M. GREGG[1], AND KEVIN L. SHELTON[2]
[1] Department of Geology and Geophysics, University of Missouri–Rolla, Rolla, Missouri 65409, U.S.A.
[2] Stable Isotope Geology and Geochemistry Group, Department of Geological Sciences, University of Missouri–Columbia, Columbia, Missouri 65211, U.S.A.

ABSTRACT: **The Trenton and Black River Limestones are dolomitized extensively along the axis of the Kankakee Arch in Indiana, with the proportion of dolomite decreasing to the south and southeast of the arch. Planar and nonplanar dolomite replacement textures and rhombic (type 1) and saddle (type 2) void-filling dolomite cements are present. Three stages of dolomitization, involving different fluids, are inferred on the basis of petrographic and geochemical characteristics of the dolomites.**

Nonferroan planar dolomite has relatively high $\delta^{18}O$ values (−1.8 to −6.1‰ PDB) and has $^{87}Sr/^{86}Sr$ ratios (0.70833 to 0.70856) that overlap those of Middle Ordovician seawater. Petrography, geochemistry, and the geometry of the dolomitized body suggest that the planar dolomite was formed in Middle and Late Ordovician seawater during the deposition of the overlying Maquoketa Shale. Ferroan planar and nonplanar dolomite occurs in the upper few meters of the Trenton Limestone, confined to areas underlain by planar dolomite. This dolomite contains patches of nonferroan dolomite with cathodoluminescence (CL) characteristics similar to underlying planar dolomite. Ferroan dolomite has relatively low $\delta^{18}O$ values (−5.1 to −7.3‰ PDB) and has slightly radiogenic $^{87}Sr/^{86}Sr$ ratios (0.70915 to 0.70969) similar to those obtained for the overlying Maquoketa Shale. These data indicate that ferroan dolomite formed by neomorphism of nonferroan planar dolomite as fluids were expelled from the overlying Maquoketa Shale during burial. The absence of ferroan dolomite at the Trenton–Maquoketa contact, in areas where the earlier-formed nonferroan planar dolomite also is absent, indicates that the fluid expelled from the overlying shale did not contain enough Mg^{2+} to dolomitize limestone.

Type 1 dolomite cement has isotopic compositions similar to those of the ferroan dolomite, suggesting that it also formed from shale-derived burial fluids. CL growth zoning patterns in these cements suggest that diagenetic fluids moved stratigraphically downward and toward the southeast along the axis of the Kankakee Arch. Type 2 saddle dolomite cements precipitated late; their low $\delta^{18}O$ values (−6.0 to −7.0‰ PDB) are similar to those of the type 1 dolomite cement. However, fluid-inclusion data indicate that the saddle dolomite was precipitated from more saline, basinal fluids and at higher temperatures (94° to 143°C) than the type 1 cements (80° to 104°C). A trend of decreasing fluid-inclusion homogenization temperatures and salinities from the Michigan Basin to the axis of Kankakee Arch suggests that these fluids emerged from the Michigan Basin after precipitation of type 1 cement.

INTRODUCTION

The Trenton and Black River Limestones in northern Indiana (Fig. 1) and adjacent states are important hydrocarbon reservoirs. Oil and gas are concentrated in areas with exceptionally high porosity development due to dissolution and extensive dolomitization along linear fracture zones, in fields such as the Albion–Scipio, Stoney Point, and Northville fields in Michigan and the Dover fields in southwestern Ontario. The Trenton and Black River Limestones also are productive in the Findlay–Lima field as well as several smaller fields in northwestern Ohio (Taylor and Sibley 1986; Hurley and Swager 1991; Coniglio et al. 1994). The lateral equivalent of these rock units on the Wisconsin and Kankakee Arches (Fig. 1), which forms the western and southwestern boundaries of the Michigan Basin, host zinc and lead sulfide deposits of the Upper Mississippi Valley Mineral District (Gregg and Sibley 1984).

Although there has been exploration for both hydrocarbons and minerals in northern Indiana, there has been relatively little recent research on the diagenesis of the Trenton and Black River Limestones in this key area (an exception is Fara and Keith 1989). The aim of this study is to establish the extent of the regional paleofluid flow system that resulted in extensive dolomitization on the Kankakee Arch area in northern Indiana. This study provides a link among relatively recent work on the Trenton–Black River in neighboring states (e.g., Gregg and Sibley 1984; Taylor and Sibley 1986; Haefner et al. 1988; Hurley and Budros 1990; Granath 1991; Budai and Wilson 1991; Coniglio et al. 1994).

REGIONAL GEOLOGIC SETTING

The Kankakee Arch in northern Indiana (Fig. 1), a southeastern extension of the Wisconsin Arch, began to form near the end of Canadian time (Early Ordovician), separating the Michigan Basin from the Illinois Basin (Collinson et al. 1988; Kolata and Nelson 1990). The arch formed a relative topographic high within a regional epeiric sea during deposition of the Trenton and Black River Limestones in the Great Lakes region (Keith 1989).

The Black River Limestone conformably overlies the St. Peter Sandstone or Glenwood Formation of the Ancell Group in the Kankakee Arch area (Fig. 2). The Black River Limestone consists of bioturbated lime mudstone, wackestone, and packstone with some grainstone beds. The upper boundary of the Black River Limestone is placed at the upward transition into limestone with a lower mud content and a higher grain content, characteristic of the Trenton. The Black River Limestone, as observed in this study, has relatively constant thickness of about 50 to 60 m along the Kankakee Arch.

The Trenton Limestone conformably overlies the Black River Limestone (Fig. 2). Original limestone fabrics are more difficult to determine in the Trenton, because it has been extensively dolomitized along the Arch except in the southeastern part of the study area. The Trenton Limestone is more grain-rich than the Black River Limestone. Crinoid, bryozoan, mollusk, and trilobite debris are common. In completely dolomitized sections, the presence of crinoid ghosts and gastropod-moldic porosity indicate similar lithologies. There is no evidence of lateral sedimentary facies changes in the Trenton Limestone along the Kankakee Arch. The Trenton Limestone is interpreted to have been deposited on a carbonate ramp under shallow-water open-marine conditions (Fara and Keith 1989). The thickness of the Trenton Limestone, as observed in this study, is about 50 to 60 m, and remains relatively constant along the Arch.

A number of researchers, using outcrop and core samples, have concluded that the contact between the Trenton Limestone and the overlying Maquoketa Shale on the southern margin of the Michigan Basin represents subaerial exposure after Trenton deposition (Rooney 1966; Taylor and Sibley 1986; DeHaas and Jones 1989). However, Keith (1985) and Keith and Wickstrom (1993) concluded that this contact actually is a submarine hardground rather than a subaerial exposure surface. We observed that the contact of the Trenton with the overlying shale is relatively sharp, with a few centimeters of relief, and is characterized by abundant pyrite minerali-

* Present address: Polar Research Center, Korea Ocean Research and Development Institute, Ansan P.O. Box 29, Seoul 425-600, Korea.

JOURNAL OF SEDIMENTARY RESEARCH, VOL. 70, NO. 1, JANUARY, 2000, P. 265–274
 1073-130X/00/070-265/$03.00

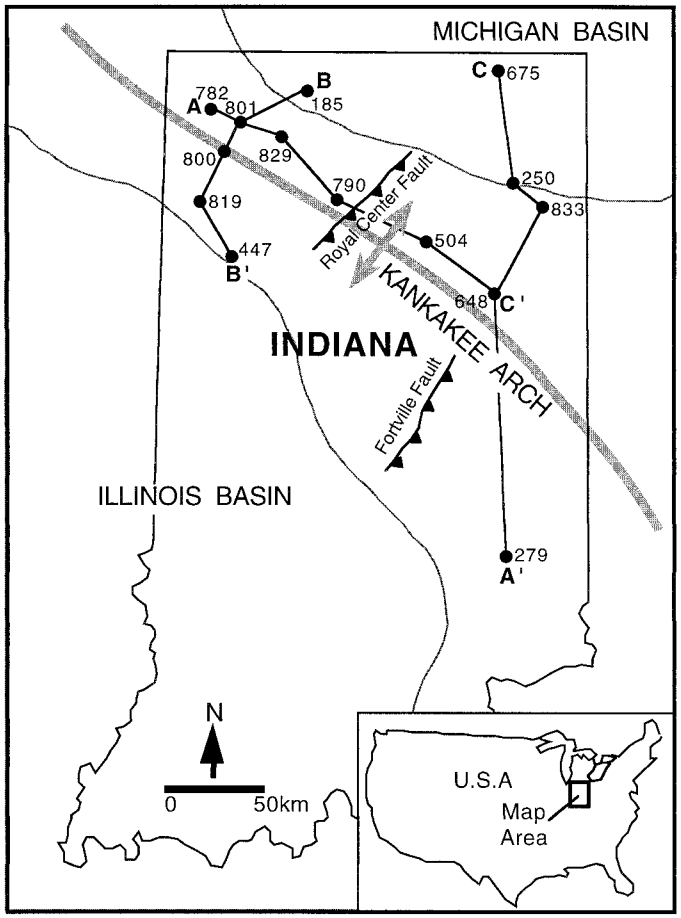

FIG. 1.—Location of the study area relative to the Michigan and Illinois Basins and the Kankakee Arch. Dots indicate locations of mineral exploration cores studied, and the location of cross sections are shown. Several large northeast-trending normal faults also are shown.

zation (up to 3 cm thick) and a concentration of phosphatic debris. There is no bleaching or evidence of karst development. The Maquoketa Shale contains dolomitized intraclasts eroded from the underlying Trenton Limestone at its base. These features, taken together, indicate that the contact between the Trenton Limestone and the overlying Maquoketa Shale is an extensively developed submarine hardground surface as suggested by previous research (Keith 1985; Fara and Keith 1989; Keith and Wickstrom 1993).

The Cincinnatian (Upper Ordovician) Maquoketa Shale has a wedge-like geometry that developed as it prograded westward from the Taconic highlands across Indiana, Illinois, and Iowa. Deposition occurred on a broad platform within a shallow epicontinental sea (Kolata and Graese 1983). Approximately 240 m of interbedded shale and limestone were deposited on the southeastern part of the Kankakee Arch area, thinning to about 60 m in the northwestern part of the Arch (Kolata and Graese 1983; Guthrie and Pratt 1994).

METHODS

A total of 363 samples of the Trenton and Black River Limestone were collected from 14 subsurface mineral exploration cores (Fig. 1) obtained from the Indiana Geological Survey. Petrographic analyses were conducted on thin sections stained with alizarin red–S and potassium ferricyanide (Dickson 1966). Cathodoluminescence (CL) properties of selected polished thin sections were examined using a Technosyn 8200 MkII apparatus operated at an accelerating voltage of approximately 11 kV with beam currents of between 150 and 250 μA. Elemental analyses were made using a computer-automated JEOL T330A scanning electron microscope (SEM), equipped with backscattered electron imagery and Kevex Quantum automated energy dispersive spectrometry, operated at 25 kV and 0.5 mA, using maximum counting times of 100 s. Spots were analyzed for Ca, Mg, Fe, and Mn using self-standardization techniques.

SYSTEM		NORTH AMERICAN SERIES/STAGE		Ma	NORTHERN INDIANA ROCK UNITS
ORDOVICIAN	Upper	CINCINNATIAN	RICHMONDIAN	438	MAQUOKETA SHALE
			MAYSVILLIAN		
			EDENIAN		
	Middle	CHAMPLAINIAN	SHERMANIAN		TRENTON LIMESTONE
			KIRKFIELDIAN		
			ROCKLANDIAN		
			BLACKRIVERIAN		BLACK RIVER LIMESTONE
			CHAZYAN		ANCELL GROUP
			WHITEROCKIAN	478	
	Lower	CANADIAN		505	PRAIRIE du CHIEN GROUP

FIG. 2.—Ordovician stratigraphy of the Kankakee Arch area, northern Indiana; adapted from Fisher et al. (1988).

Microthermometric measurements of fluid inclusions were performed on a Fluid Inc. gas-flow-type heating–freezing stage. Temperatures of homogenization (T_h) and last ice melting (T_m) have standard errors of ± 1°C and ± 0.2°C, respectively. Salinities for fluid inclusions were calculated based on freezing point depression in the system H_2O–NaCl (Potter et al. 1978).

Determination of carbon and oxygen isotopic compositions were made on selected dolomite crystals or groups of crystals and calcite micrite drilled from rock chips from which thin sections were prepared. Dolomite and calcite were reacted at 25°C with phosphoric acid. Data are reported in standard δ notation relative to PDB for C and O. The standard error of each analysis is less than ± 0.05‰. The $\delta^{18}O$ values were corrected by 0.8‰ for differences in acid fractionation of dolomite and calcite (McCrea 1950; Friedman and O'Neil 1977). Strontium-isotope compositions of selected dolomite crystals were analyzed at University of Texas at Dallas. Analytical error in measured $^{87}Sr/^{86}Sr$ ratio is ± 0.00009 (2σ), based on reproducibility of NBS-987 samples.

RESULTS

Dolomite Geometry

Analysis of cores indicate that the combined thickness of the Trenton and Black River Limestones along the Kankakee Arch is about 100 to 110 m. No significant lateral variation in original limestone lithologies were observed across the study area, and dolomite distribution does not appear to be related to the depositional facies. The geometry of the dolomite body is wedge-shaped, tapering to the south and southeast along of the axis of the Arch (Fig. 3). Dolomite also grades into undolomitized limestone, over distances of tens of kilometers on the northern and southern flanks of the arch, into the Michigan and Illinois Basins, respectively (Fig. 3). Stratigraphic sections examined on the northwestern part of the Arch are completely dolomitized, whereas the volume of dolomite decreases gradually upsection towards the southeast. The boundary between dolomite and the underlying limestone is gradational.

Petrography

Dolomite in the Trenton and Black River Limestones is fabric nonselective relative to sedimentary facies. Two distinct types of replacement dolomite were observed in the Trenton and Black River Limestones: nonferroan planar dolomite and ferroan dolomite that displays both planar and nonplanar texture (classification system of Sibley and Gregg 1987). Two types of open-space-filling dolomite cement also were observed: equant rhombs (type 1), and saddle dolomite (type 2).

Nonferroan Planar Dolomite.—Nonferroan planar-e and planar-s dolomite crystals range in size from 0.03 to 0.5 mm (Fig. 4A). Dolomite crystal size decreases downward in the section, with the smallest crystals replacing mud-rich precursor lithologies of the Black River Limestone. Planer-e dolomite is interpreted to have replaced grain-rich and porous precursor limestone lithologies, whereas the planar-s dolomite replaced mud-rich precursor limestones. Planar dolomites commonly have cloudy cores and clear rims (Fig. 4A).

At and below gradational dolomite–limestone contacts, patches of planar dolomite and individual planar dolomite crystals commonly are associated with burrows and stylolites. These crystals commonly exhibit dedolomitization along their edges and

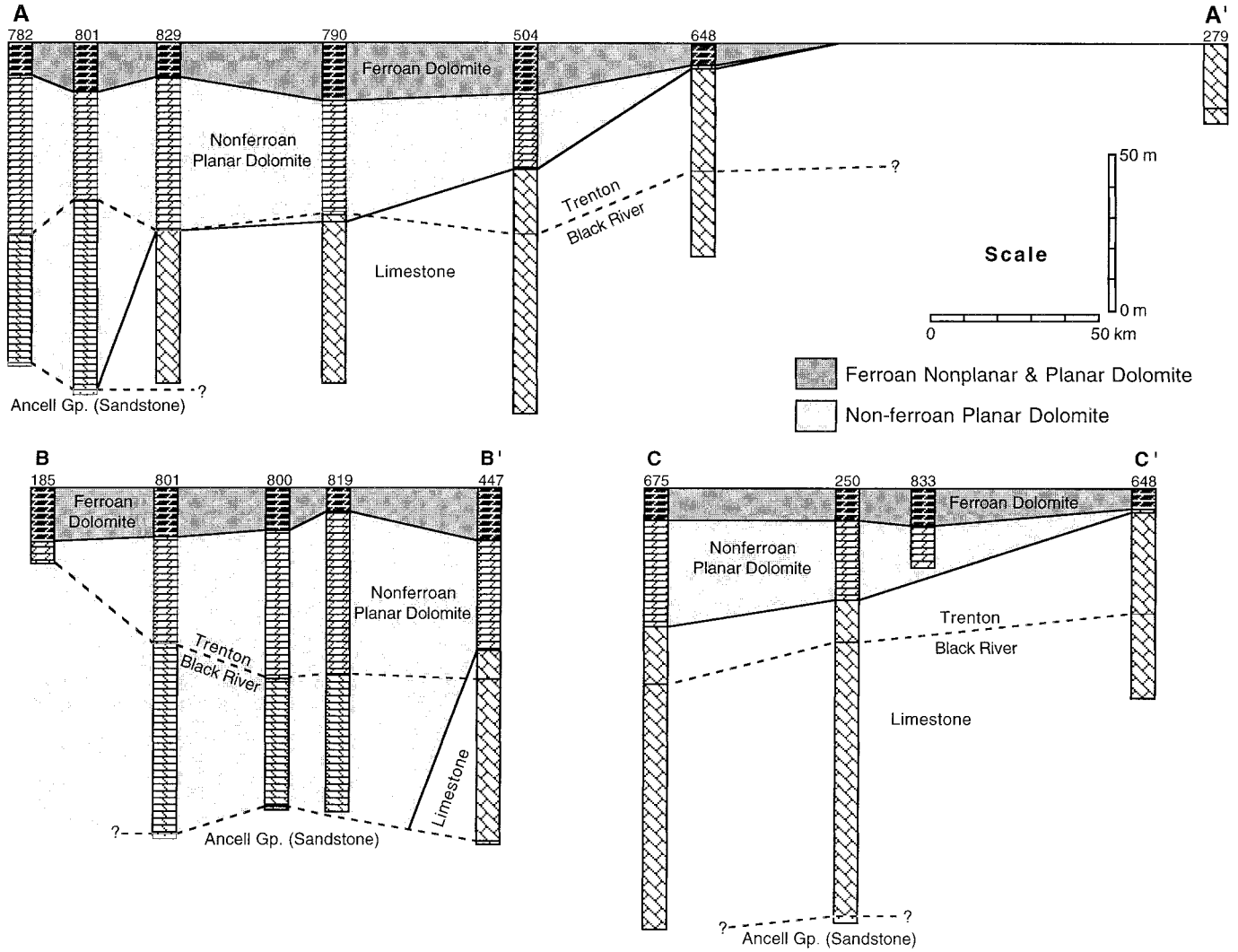

FIG. 3.—Stratigraphic sections A–A′, B–B′, and C–C′ showing distribution of nonferroan planar and ferroan nonplanar and planar dolomites. See Figure 1 for locations.

within their cores but are otherwise similar petrographically to dolomite crystals in the overlying completely dolomitized sections.

The nonferroan planar dolomite ranges from non-CL to bright red, most commonly a uniform brown-red CL (Fig. 4B). Clear rim–cloudy core planar crystals, in the upper part of the section, display dark brown CL cores and non-CL rims.

Ferroan Dolomite.—Ferroan dolomite occurs in the upper 6 to 20 m of the dolomitized Trenton section directly underlying the Maquoketa shale (Fig. 3), corresponding with the ''cap dolomite'' of Taylor and Sibley (1986) in the Michigan Basin. Ferroan nonplanar dolomite crystals range in size from 0.05 to 0.5 mm (Fig. 4C). Semiquantitative SEM-EDS analysis indicates an average content of approximately 1.5 to 2 mole % $FeCO_3$. Iron content is highest at the contact with the Maquoketa Shale, and decreases downward.

Near the contact with the overlying Maquoketa Shale, this dolomite displays uniform dark brown CL to non-CL (Fig. 4D). The intensity of CL increases down section, ranging from dark brown to dull red CL. This section contains occasional patches of dolomite with uniform bright red CL similar to that exhibited by the underlying planar dolomite (Fig. 4D). ''Ghosts'' of fossil crinoids commonly are observed in the nonplanar dolomite section by their slightly brighter CL.

Ferroan planar-e dolomite occasionally occurs in zones of high porosity, associated with ferroan nonplanar dolomite. Ferroan planar-e dolomite has a range of crystal sizes similar to that of ferroan nonplanar dolomite, displays undulatory extinction, and forms irregular compromise boundaries more commonly than the underlying nonferroan planar dolomite. Ferroan planar dolomite largely shows non-CL to dark brown CL.

Type 1 Cement.—This dolomite cement occurs as void-filling equant rhombs that display uniform extinction in cross-polarized light. It fills intercrystal pores, vugs, dissolution-enlarged fractures, and moldic pores (Fig. 5A). Type 1 dolomite cement is zoned with respect to iron, containing up to 12 mole % $FeCO_3$. The volume of type 1 cement and the size of individual type 1 crystals decreases stratigraphically downsection and decreases southeast along the axis of the Kankakee Arch (Fig. 3). Type 1 dolomite cement commonly is followed paragenetically by porosity-occluding calcite cement, and less commonly, by anhydrite or gypsum or by pyrite and rarely by sphalerite.

In the upper part of the section type 1 dolomite cement displays a complex CL microstratigraphy resulting from Fe^{2+} and Mn^{2+} growth zoning. Two distinct CL zones occur in the cement (Fig. 5B). Zone 1 displays alternating bands ranging in luminescence from non-CL to bright red, and commonly contains one or more dissolution surfaces. The number of alternating bands in zone 1 decreases stratigraphically downsection, and this zone disappears entirely in the lower part of the dolomitized section. In the southeastern Kankakee Arch area (core 648 on Fig. 1) CL zone 1 is missing in the entire section. Zone 2 is a relatively thick outer zone of dolomite cement that displays dull-CL to non-CL.

Type 2 Cement.—This cement is composed of large, open-space-filling saddle dolomite crystals (Fig. 5C). This dolomite cement is less common than type 1 cement, and was observed only in cores 447, 504, 833, and 250 (Fig. 1). It is present in dissolution-enlarged fractures and vugs, where it grew by continued enlargement of replacement dolomite crystals on pore margins (Fig. 5C). It displays up to four alternating dull-CL and non-CL growth zones (Fig. 5D). When associated with type 1 dolomite cement, it always occurs paragenetically later and is followed paragenetically by porosity-occluding anhydrite, gypsum, and sphalerite and, rarely, by fluorite. Type 2 cement commonly is associated with bitumen and occasionally contains hydrocarbon inclusions.

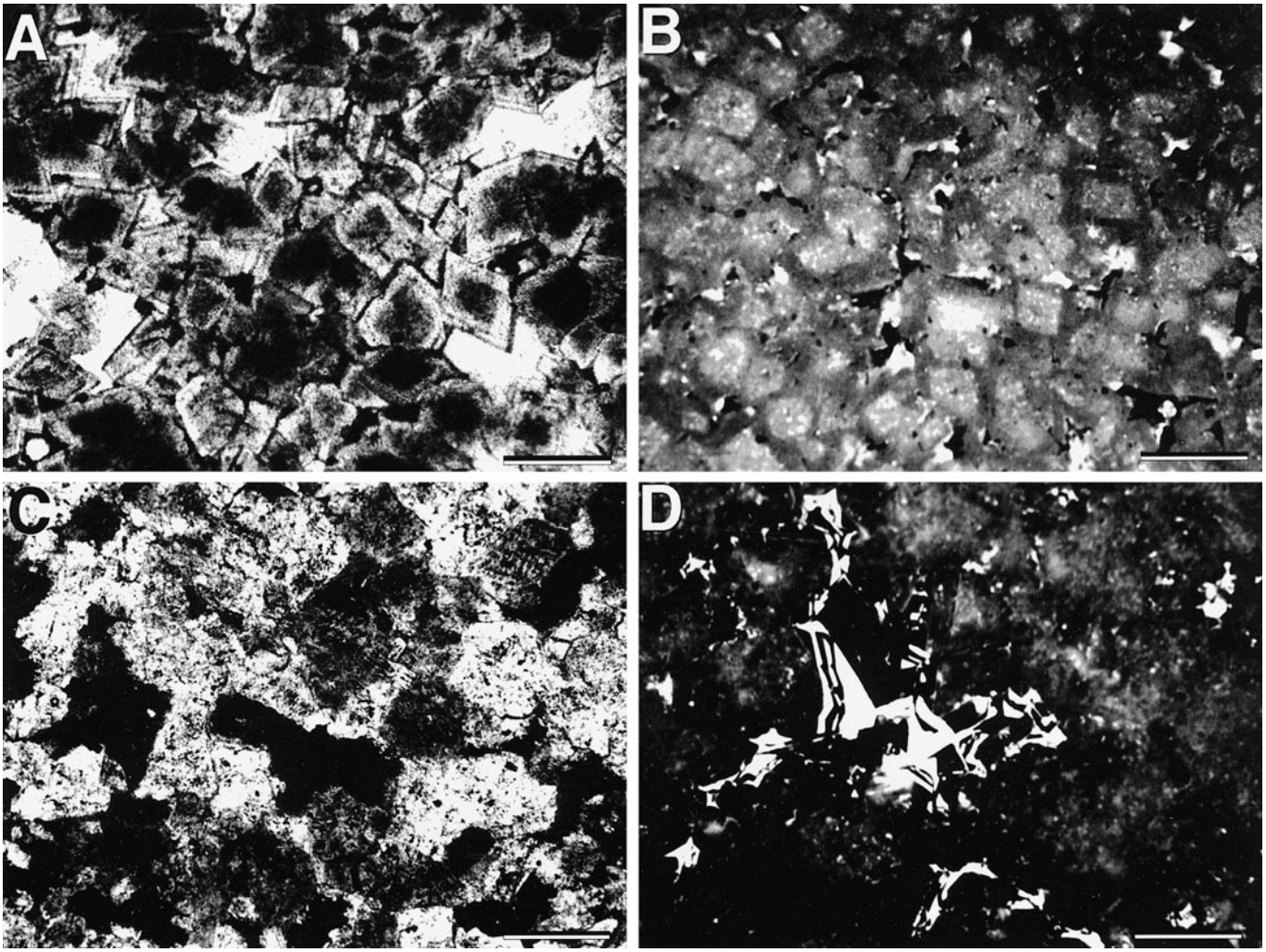

FIG. 4.—Photomicrographs of replacement dolomites. **A)** Nonferroan planar-e dolomite showing cloudy core and clear rim texture. Plane-polarized light. **B)** Cathodoluminescence photomicrograph of nonferroan planar-e dolomite (different field than in Part A). Cloudy core shows brighter CL than clear rim. **C)** Ferroan nonplanar dolomite. Cross-polarized light. **D)** Cathodoluminescence photomicrograph of ferroan nonplanar dolomite (same field as C) revealing type 1 dolomite cement (center). Some bright CL patches remain within otherwise quenched-CL nonplanar dolomite. Scale bars = 0.2 mm.

Geochemistry

Stable-Isotope Compositions.—The $\delta^{18}O$ and $\delta^{13}C$ values for the various types of dolomite and associated micritic calcites are shown in Figure 6 and Table 1. The four $\delta^{18}O$ values of micritic calcites from the lime mudstones in the Trenton and Black River Limestones display a small range from -3.9 to -4.7‰ with a mean of -4.3‰ (PDB). The $\delta^{13}C$ values range from $+1.4$ to -0.8‰ with an average of 0.0‰ (PDB). These values are similar to those of North American Upper Ordovician marine calcite but lower with respect to $\delta^{18}O$ than Middle Ordovician marine calcite (Lohmann 1988; Lohmann and Walker 1989).

The $\delta^{18}O$ and $\delta^{13}C$ values of replacement dolomites cluster in two distinct groups (Fig. 6). Planar dolomite crystals have higher $\delta^{18}O$ and $\delta^{13}C$ values than nonplanar dolomite. They also have a wider range of $\delta^{18}O$ (-1.8 to -6.1‰) and $\delta^{13}C$ ($+0.6$ to -1.5‰) values relative to nonplanar dolomite ($\delta^{18}O = -5.1$ to -7.3‰, $\delta^{13}C = -0.7$ to -2.1‰). The stable-isotope values of both types of replacement dolomite display no systematic variation with stratigraphy or with geographic location (Table 1).

The range of $\delta^{18}O$ and $\delta^{18}C$ values of type 1 dolomite cement are -5.2 to -6.8‰ and $+0.9$ to -1.4‰, respectively. The range of $\delta^{18}O$ values of type 1 cement overlaps with that of replacement dolomite. The $\delta^{18}O$ and $\delta^{18}C$ values of type 2 saddle dolomite cement plot in a relatively narrow range of -6.0 to -7.0‰ and $+0.3$ to -0.6‰, respectively, and are lighter in $\delta^{18}O$ than type 1 cement on the average.

Radiogenic-Isotope Compositions.—The $^{87}Sr/^{86}Sr$ values of 10 selected dolomite samples are shown in Table 1 and in Figure 7 together with their corresponding $\delta^{18}O$ values. Three samples of planar dolomite have $^{87}Sr/^{86}Sr$ ratios between 0.70833 to 0.70856. One sample collected directly below the boundary with the overlying ferroan nonplanar dolomite yielded a higher $^{87}Sr/^{86}Sr$ ratio of 0.70902. Nonplanar dolomites have higher $^{87}Sr/^{86}Sr$ ratios (0.70915 to 0.70969) than planar dolomites. The scatter of Sr values may be due, in part, to minor clay contamination, although the rocks are largely nonargillaceous. One sample of type 1 dolomite cement has a $^{87}Sr/^{86}Sr$ ratio of 0.70897, which is close to that of nonplanar dolomite. One analysis of type 2 saddle dolomite cement has a relatively low $^{87}Sr/^{86}Sr$ ratio of 0.70833.

Fluid Inclusions.—Microthermometric measurements were made on 81 primary fluid inclusions in samples of type 1 (14) and type 2 (67) dolomite cements (Table 2). All of the inclusions are two-phase (liquid-rich with vapor bubble) and display a rectangular to slightly irregular shape (Fig. 8). Fluid inclusions observed in type 1 cements are very small, ranging from 2 to 10 μm in the longest axis, and contain a small vapor bubble composing less than 10 volume %, which is active at room temperature (Fig. 8A). Fluid inclusions in type 2 saddle dolomite cements range from <4 to 30 μm in the longest axis and contain a vapor bubble constituting <10 to 20 volume % of each inclusion (Fig. 8B). Occasional liquid hydrocarbon inclusions were observed in type 2 cement; these are distinguished by a slight brownish color and bright greenish-yellow fluorescence under ultraviolet light (Fig. 8C, D).

Fluid inclusions in type 1 cements filling cavities in planar dolomites exhibit a narrow range of T_h values from 80° to 104°C, averaging 83°C. Last ice-melting

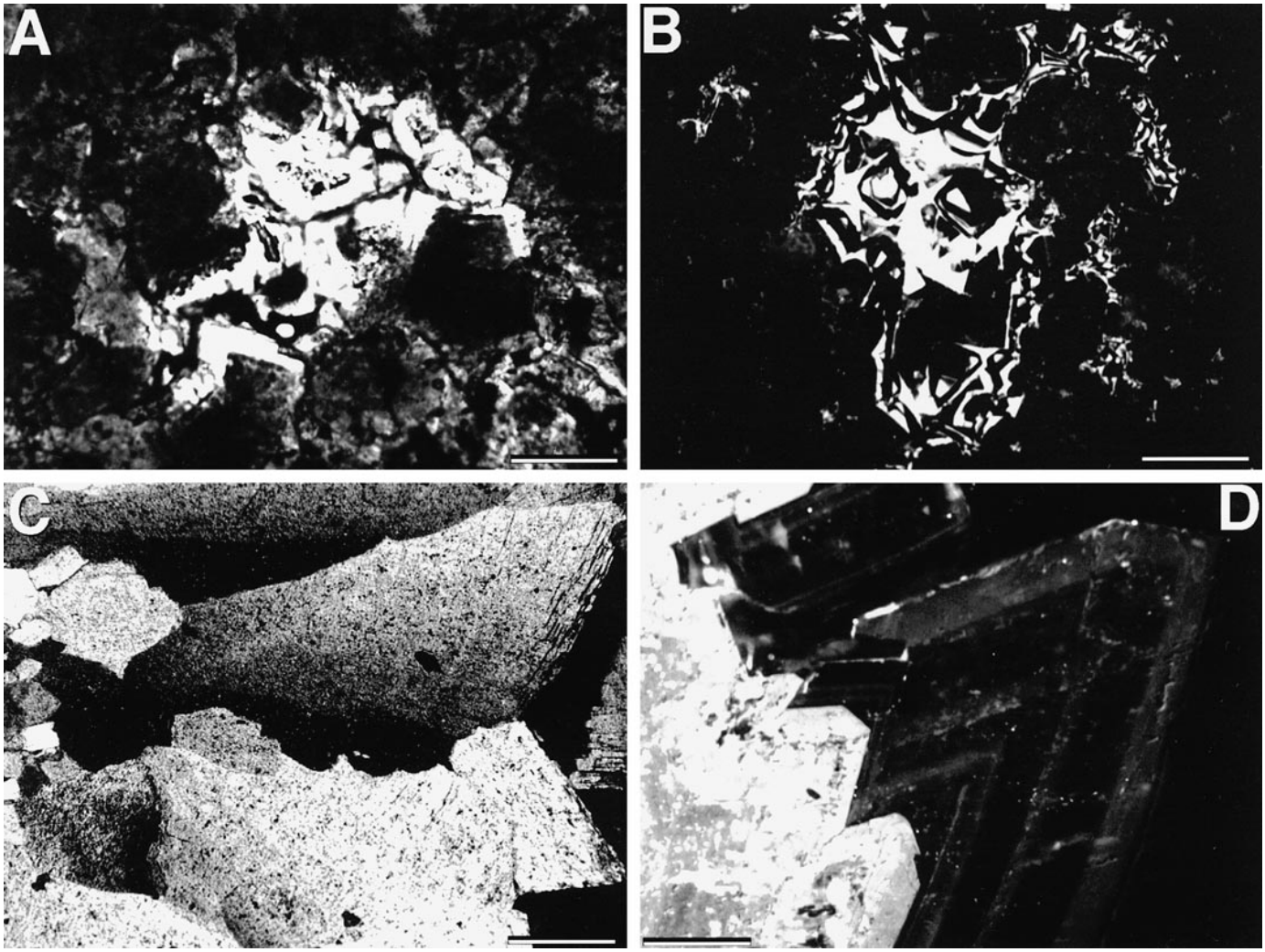

FIG. 5.—Photomicrographs of dolomite cements. **A)** Type 1 dolomite cement precipitated in vuggy porosity as overgrowth on replacement dolomite. Plane-polarized light. **B)** Type 1 dolomite cement showing 2-zone CL pattern of (1) inner alternating non-CL to bright red bands and (2) outer thick non-CL zone. **C)** Type 2 (saddle) dolomite cement. Cross-polarized light. **D)** Saddle dolomite CL pattern consisting of three alternating dull-CL and non-CL zones (occasionally up to four alternating zones are visible) on a substratum of nonferroan planar dolomite. Scale bars = 0.2 mm.

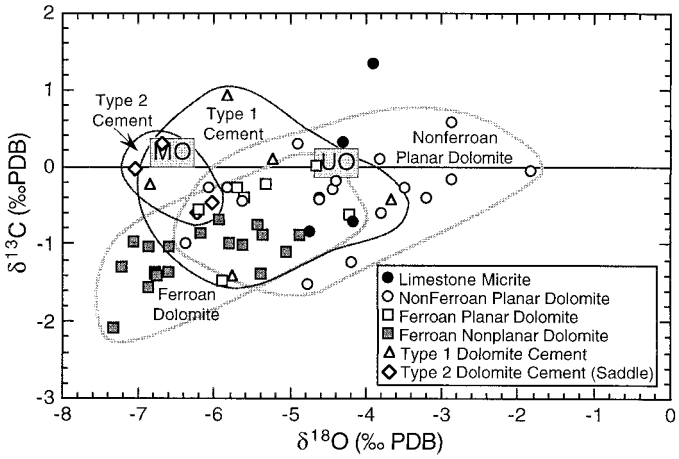

FIG. 6.—$\delta^{18}O$ and $\delta^{13}C$ values of replacement dolomites, dolomite cements, and calcite micrite from the Trenton and Black River Limestones. Larger rectangles are the estimated values for marine calcite precipitated from Middle Ordovician (MO) and Upper Ordovician (UO) seawaters (Lohmann 1988; Lohmann and Walker 1989).

temperatures (freezing-point depression) of these fluid inclusions range from −13.7 to −0.8°C (average, −6.2°C), indicating salinities between 17.7 and 1.4 weight % NaCl equivalent (Potter et al. 1978). T_h values of fluid inclusions in type 2 saddle dolomite cement show a larger range of values from 94° to 143°C, averaging 118°C. First melting temperatures of these inclusions range from −54.4° to −47.5°C, indicating that the inclusion fluids are complex Na–Ca–K–Cl brines (Crawford 1981). Last ice-melting temperatures range from −31.6° to −11.2°C, averaging −21.8°C. These values indicate salinities of about 30.2 to 15.2 weight % NaCl equivalent (Potter et al. 1978). Homogenization temperatures and salinities of fluid inclusions in saddle dolomite display a weak trend of higher values near the Michigan Basin that decrease away from the basin (Table 2, Fig. 9).

DOLOMITIZATION OF THE TRENTON AND BLACK RIVER LIMESTONES

Petrographic and geochemical data of Trenton and Black River dolomites in the context of the regional geology allow us to evaluate the dolomitization mechanisms and to infer the paleoflow paths of the dolomitizing fluids. Three stages of dolomitization (Fig. 10), each associated with different dolomitizing fluids, are hypothesized.

Early Diagenesis

The nonferroan planar dolomites of this study have petrographic and geochemical characteristics identical with ''regional dolomite'' described in other studies of the

TABLE 1.—*Carbon, oxygen and strontium isotope data.*

Core and Sample #	Depth (meters)	Lithology	$\delta^{13}C$ (‰PDB)	$\delta^{18}O$ (‰PDB)	$^{87}Sr/^{86}Sr$
Top of Trenton	309.4				
648-3	309.8	Fe nonplanar dolomite	−2.08	−7.34	0.70915
648-5	311.2	Fe planar dolomite	0.01	−4.66	0.70852
648-7	316.3	Fe planar dolomite	−0.22	−5.32	
Top of Black River	364.0				
648-15	371.6	limestone micrite	0.33	−4.31	
Top of Trenton	325.6				
790-2	325.9	Fe nonplanar dolomite	−1.04	−6.87	0.70924
790-7	334.8	Fe nonplanar dolomite	−1.37	−6.60	
790-9	342.2	Fe planar dolomite	−0.27	−5.70	
790-10	347.2	non-Fe planar dolomite	−0.45	−5.63	0.70856
790-13	375.5	non-Fe planar dolomite*	−0.26	−5.83	
Top of Black River	379.9				
790-19	406.8	limestone micrite	−0.84	−4.74	
Top of Trenton	362.8				
801-2	363.5	Fe nonplanar dolomite	−1.42	−6.77	
801-7	368.1	Fe nonplanar dolomite	−0.96	−7.08	0.70969
801-12	377.0	Fe nonplanar dolomite	−1.30	−7.22	
801-18	398.8	low-Fe nonplanar dolomite	−1.39	−6.78	
Top of Black River	412.5				
801-28	424.4	non-Fe planar dolomite	−0.29	−4.44	0.70833
801-42	463.2	non-Fe planar dolomite	−0.41	−3.21	
Top of Trenton	338.7				
829-2	339.0	Fe nonplanar dolomite	−1.39	−5.40	
829-5	344.6	Fe nonplanar dolomite	−0.89	−4.88	
829-7	349.7	non-Fe planar dolomite	−1.52	−4.78	
829-11	365.1	non-Fe planar dolomite	−1.00	−6.39	
829-14	380.3	non-Fe planar dolomite*	−0.40	−4.62	
829-14	380.3	non-Fe planar dolomite	−0.42	−4.62	
Top of Black River	397.9				
829-25	442.5	limestone micrite	−0.71	−4.18	
Top of Trenton	325.0				
504-3	325.7	Fe nonplanar dolomite	−1.37	−6.78	
504-8	332.4	Fe planar dolomite	−0.56	−6.21	
504-14	352.0	non-Fe planar dolomite	0.29	−4.90	
504-16	360.6	Type-1 dolomite cement	0.10	−5.23	
504-17	362.0	non-Fe planar dolomite	−0.27	−6.07	
504-23	381.4	limestone micrite	1.35	−3.90	
Top of Black River	385.4				
Top of Trenton	299.7				
447-1	299.7	Fe nonplanar dolomite	−1.55	−6.87	
447-5	302.9	non-Fe planar dolomite	−0.16	−2.87	
447-8	312.5	non-Fe planar dolomite	−0.59	−3.80	
447-8	312.5	Type-1 dolomite cement	−1.40	−5.76	0.70897
447-12	329.3	non-Fe planar dolomite*	0.11	−3.83	
Top of Black River	360.7				
Top of Trenton	398.4				
185-3	399.1	Fe nonplanar dolomite	−0.98	−5.81	
185-6	401.6	Fe nonplanar dolomite	−0.87	−6.19	
185-11	411.6	Fe nonplanar dolomite	−1.11	−5.07	
185-16	421.1	low-Fe nonplanar dolomite	−0.68	−5.94	
Top of Trenton	279.3				
819-3	279.9	Fe planar dolomite	−1.47	−5.90	
819-8	287.5	non-Fe planar dolomite	−1.22	−4.20	
819-16	309.5	non-Fe planar dolomite	−0.28	−3.50	
Top of Black River	335.4				
Top of Trenton	292.1				
782-1	292.1	Fe nonplanar dolomite	−0.76	−5.43	
782-3	293.4	Fe nonplanar dolomite	−0.89	−5.38	0.70957
782-10	302.9	low-Fe nonplanar dolomite	−1.02	−5.63	
782-16	325.0	non-Fe planar dolomite	−0.18	−4.40	
782-20	348.6	non-Fe planar dolomite	0.59	−2.88	0.70902
782-21	350.6	Type-1 dolomite cement	−0.42	−3.67	
Top of Black River	352.4				
782-30	380.0	non-Fe planar dolomite	−0.06	−1.83	
Top of Trenton	473.4				
833-2	473.8	Fe planar dolomite	−0.39	−5.61	
833-3	474.6	Fe nonplanar dolomite	−1.04	−6.61	
833-7	478.6	Fe planar dolomite	−0.61	−4.21	
833-9	480.5	Type-2 dolomite cement	−0.47	−6.03	
833-12	485.5	Type-2 dolomite cement	−0.59	−6.22	
Top of Trenton	499.4				
250-7	517.0	Type-1 dolomite cement	−0.23	−6.84	
250-9	518.1	Type-2 dolomite cement	0.30	−6.70	
250-10	519.7	Type-1 dolomite cement	0.94	−5.83	
250-12	532.9	Type-2 dolomite cement	−0.03	−7.04	0.70833
Top of Black River	548.5				

* Sample contained significant Type-1 dolomite cement.

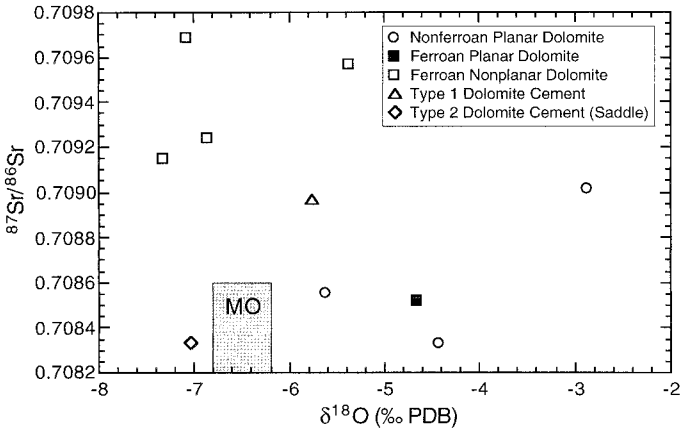

FIG. 7.—$^{87}Sr/^{86}Sr$ ratio vs. $\delta^{18}O$ values of replacement dolomites and dolomite cements. Large rectangle encloses the estimated strontium isotope value of Middle Ordovician seawater (Burke et al. 1982) and the estimated $\delta^{18}O$ value of marine calcite precipitated from Middle Ordovician seawater (Lohmann 1988; Lohmann and Walker 1989).

Michigan Basin and surrounding areas (Taylor and Sibley 1986; Fara and Keith 1989; Budai and Wilson 1991). The regional dolomite is characterized by its nonferroan composition relative to ferroan ''cap dolomite'', and occurs on the western and southwestern sides of the Michigan Basin (Taylor and Sibley 1986; Budai and Wilson 1991) and in the lower part of the Trenton Formation in northern Indiana (Fara and Keith 1989). In the Michigan Basin, geographic confinement to an area adjacent to the Wisconsin Arch, to the northwest of the study area, and lower $\delta^{18}O$ values of regional dolomite led to an interpretation that this dolomite was formed by mixture of seawater and meteoric water recharged from the arch area (Budai and Wilson 1991). Taylor and Sibley (1986) suggested that the regional dolomite formed at or near the earth's surface during early diagenesis. Fara and Keith (1989) instead suggested that the regional dolomite in northern Indiana formed from basinal fluids during deep burial of the Trenton and Black River Limestones.

Our evidence leads us to conclude that planar dolomite was formed by seawater during early diagenesis. Although the Kankakee Arch remained a topographic high relative to surrounding basins after its initial formation, there is no evidence of subaerial exposure during or after deposition of the Trenton and Black River Limestones (e.g., Keith 1985; Keith and Wickstrom 1993; and this study). If the arch area experienced subaerial exposure and meteoric water had been available, then the planar dolomite body might show a wedge shape tapering toward the surrounding basins from the axis of the Kankakee Arch, as does the Galena Group dolomite on the Wisconsin Arch (e.g., Badiozamani 1973). However, the geometry of the dolomite body in northern Indiana displays a ''wedge-shaped'' geometry, tapering upwards toward the south and southeast along the crest of the Kankakee Arch. The Trenton and Black River Limestones southeast along the Kankakee Arch are largely undolomitized (Fig. 3).

We suggest the following possible mechanism for the formation of the dolomite. As deposition of the overlying Maquoketa Shale commenced and prograded westward during Late Ordovician time (Cook and Bally 1975; Kolata and Graese 1983), dolomitization was initiated via influx of Mg-rich seawater into the underlying Trenton and Black River Limestones (Fig. 10A). Nonferroan planar dolomite began to form as this fluid migrated downward at and prior to time T_1 (Fig. 10A), forming dolomite body Dt_1. The hydrologic drive for fluid flow possibly was thermal buoyancy and/or other as yet unknown mechanisms (e.g., Land 1991). At time T_2 shale deposition had prograded farther to the northwest and acted as a barrier to downward influx of water and the dolomitizing front receded to the northwest along the axis of the arch. This resulted in dolomite body Dt_2 with a lateral limestone contact to the northwest of dolomite body Dt_1. By time T_3 shale deposition had prograded even farther westward, resulting in continuing northwest retreat of dolomitizing fluids (dolomite body Dt_3) (Fig. 10A).

The petrographic texture of the planar dolomite is typical of dolomites formed under relatively near-surface, low-temperature conditions (Sibley and Gregg 1987). The $\delta^{18}O$ values of planar dolomite vary from values close to Middle Ordovician marine calcite to up to 3‰ heavier than Upper Ordovician marine calcite (Fig. 6). Estimates of calcite–dolomite oxygen isotope fractionation at 25°C predict that dolomite might have $\delta^{18}O$ values 3 ± 1‰ higher than coexisting calcite (Land 1985). The approach toward equilibrium with Middle Ordovician seawater calcite values may indicate that Middle Ordovician seawater trapped in limestone during deposi-

TABLE 2.—*Fluid inclusion data.*

Core	Dolomite Cement Type	First Melting Temperature (T_{fm})	Final Melting Temperature (T_m)	Homogenization Temperature (T_h)
447	Type 1 Dolomite	−54.1	−9.2	79.6
			−7.2	80.7
			−7.9	81.7
			−13.7	84.8
			−1.4	85.6
			−4.2	85.6
			−9.0	88.2
			−2.5	92.3
			−12.6	94.3
			−0.8	95.6
			−0.8	96.3
			−5.5	97.2
			−6.4	103.7
			−6.2	82.6
447	Type 2 Dolomite	−53.6	−21.1	94.2
			−19.1	97.3
			−16.2	100.7
		−51.5	−20.1	102.8
			−20.3	103.7
			−21.4	106.0
			−14.1	107.2
			−22.9	111.9
		−50.2	−17.5	113.9
			−19.4	118.8
			−18.9	119.3
			−17.6	120.0
			−19.0	121.2
			−11.2	123.1
		−52.5	−23.0	123.5
			−16.1	129.3
			−19.9	130.0
504	Type 2 Dolomite		−21.8	100.7
			−19.9	107.8
			−22.3	109.3
			−23.5	121.3
250	Type 2 Dolomite		−24.1	102.4
			−18.7	103.3
			−17.2	103.5
		−52.2	−22.6	109.6
			−23.7	111.2
			−25.0	111.5
			−23.4	112.4
			−22.6	114.2
			−23.0	115.7
			−23.8	115.8
			−24.1	119.7
			−19.6	119.7
			−24.2	120.1
			−23.5	120.2
			−23.3	121.9
			−24.7	124.6
		−53.7	−22.7	124.7
			−24.9	125.1
			−25.3	125.9
			−25.2	126.1
			−25.1	127.5
		−53.2	−12.1	128.6
			−23.9	130.1
			−24.0	132.9
			−23.5	133.4
			−26.6	133.6
			−22.5	137.5
			−20.1	121.3
			−22.5	122.2
			−20.8	124.8
		−47.5	−21.5	125.1
			−21.1	125.7
		−50.5	−22.1	127.3
			−22.0	132.1
		−52.1	−21.0	132.5
		−54.4	−20.9	134.3
		−51.3	−21.6	137.5
833	Type 2 Dolomite	−53.2	−31.6	89.3
			−24.8	100.4
			−21.3	103.4
			−20.4	107.0
			−22.6	112.4
		−52.3	−25.2	112.7
			−23.5	129.2
			−23.8	135.0
			−26.2	143.2

tion played a role in controlling the geochemical characteristics of planar dolomite. The $^{87}Sr/^{86}Sr$ ratios of planar dolomite overlap that of Middle and Late Ordovician seawater (Burke et al. 1982) (Fig. 7); this is consistent with the seawater dolomitization model proposed here.

Burial (Intermediate Diagenesis)

Distribution of ferroan nonplanar dolomite and volumetrically less important ferroan planar dolomite is confined to the upper part of the Trenton Limestone in the Kankakee Arch area. The close relationship of the cap dolomite to the overlying Maquoketa Shale (= Utica Shale) and its ferroan composition was noted by Taylor and Sibley (1986), which led them to conclude that the cap dolomite postdated regional dolomitization and formed under reducing conditions in a shallow burial environment during compaction of the overlying shale. Budai and Wilson (1991) proposed that the cap dolomite was formed by seawater during an initial diagenetic stage and was later modified by higher burial temperature and/or fluids with a low $\delta^{18}O$ composition, possibly provided from the overlying Utica Shale. On the basis of its ferroan composition and preservation of primary sedimentary textures, Fara and Keith (1989) interpreted the cap dolomite in northern Indiana to have formed by reaction with Fe-rich fluids expelled from the overlying Maquoketa Shale during early compaction.

Ferroan dolomite is distributed in the upper part of the Trenton Limestone, and its volume decreases abruptly downward a few meters below the contact with the overlying Maquoketa Shale (Fig. 3). The dolomite invariably has a higher Fe^{2+} composition than earlier formed nonferroan planar dolomite. The Fe^{2+} in nonplanar dolomite was interpreted by Taylor and Sibley (1986) to have been liberated from the overlying shale by reduction of unstable iron-oxide coatings on clay minerals (Curtis 1967), ion-exchange processes in the clay lattice (Irwin 1980), and transformation of smectite to illite during burial of clay (Boles and Franks 1979; McHargue and Price 1982).

The $^{87}Sr/^{86}Sr$ ratios of ferroan nonplanar dolomite (0.70915–0.70969) are the most radiogenic among all types of dolomite in this study (Fig. 7) and indicate introduction of ^{87}Sr into the Trenton Limestone during the formation of this dolomite. Whole-rock analysis of the $^{87}Sr/^{86}Sr$ ratio of the Maquoketa Shale yielded a highly radiogenic value of 0.73434 (Stueber et al. 1987). $^{87}Sr/^{86}Sr$ ratios of 0.71023 to 0.71290 for acid leachate of the Devonian New Albany Shales, which had Sr-isotope values similar to those of the Maquoketa Shale (Stueber et al. 1987), are comparable to the ferroan nonplanar dolomite. The radiogenic Sr-isotope compositions, in conjunction with the distribution of the ferroan dolomites, indicate that fluids expelled from the Maquoketa Shale are the likely source from which the ferroan dolomite formed.

Although the Maquoketa Shale overlies the Trenton Limestone throughout the Kankakee Arch area, there is no ferroan dolomite below the Trenton–Maquoketa contact in the southeast, where early nonferroan planar dolomitization does not occur at the top of the Trenton Limestone (Fig. 10). This indicates that the diagenetic fluid expelled from the overlying shale did not contain enough Mg^{2+} to dolomitize limestone, which further suggests that the ferroan nonplanar and planar dolomites are a product of neomorphic recrystallization of preexisting nonferroan planar dolomite. The scattered distribution of bright red CL patches in the ferroan dolomite (Fig. 4D), which have CL characteristics similar to those in the underlying nonferroan planar dolomite, may be relict of unneomorphosed nonferroan planar dolomite.

Nonplanar textures typical of the ferroan dolomite are characteristic of epigenetic dolomite formed at elevated temperature (>50°C) (Gregg and Sibley 1984; Sibley and Gregg 1987). High homogenization temperatures of fluid inclusions in type 1 dolomite cement (80° to 104°C) support an epigenetic origin for the paragenetically related ferroan dolomite (see discussion below) (Fig. 9). The lower $\delta^{18}O$ values of ferroan dolomite (Fig. 6) also is consistent with this view. The variation of $\delta^{18}O$ values of nonferroan planar dolomite (Fig. 6) may also reflect the influence of descending shale-derived fluids.

The slight difference in $\delta^{13}C$ values between ferroan and nonferroan dolomites (Fig. 6) reflects the dominant control of the precursor planar dolomite phase. Possibly the slightly lower $\delta^{13}C$ values of nonplanar dolomite were influenced by ^{12}C-enriched fluids that acquired oxidized carbon during burial of the overlying organic-rich Maquoketa Shale.

Type 1 Cement.—During and after the formation of ferroan dolomite in the upper part of the Trenton Limestone, type 1 dolomite cement likely precipitated in open space in the entire dolomitized part of the section. Type 1 cements developed in planar dolomite display somewhat higher $\delta^{18}O$ values than those in nonplanar dolomite, suggesting some buffering of the precipitating fluids by the host lithology. However, their lower $\delta^{18}O$ values, by about 1 to 2‰ relative to hosting planar replacement dolomite, indicate a different fluid from that which formed the host dolomite. Isotopic signatures of type 1 cement similar to those of ferroan dolomite (Figs. 6, 7) and relatively high Fe content suggest that both dolomites were formed from the same or similar diagenetic fluids.

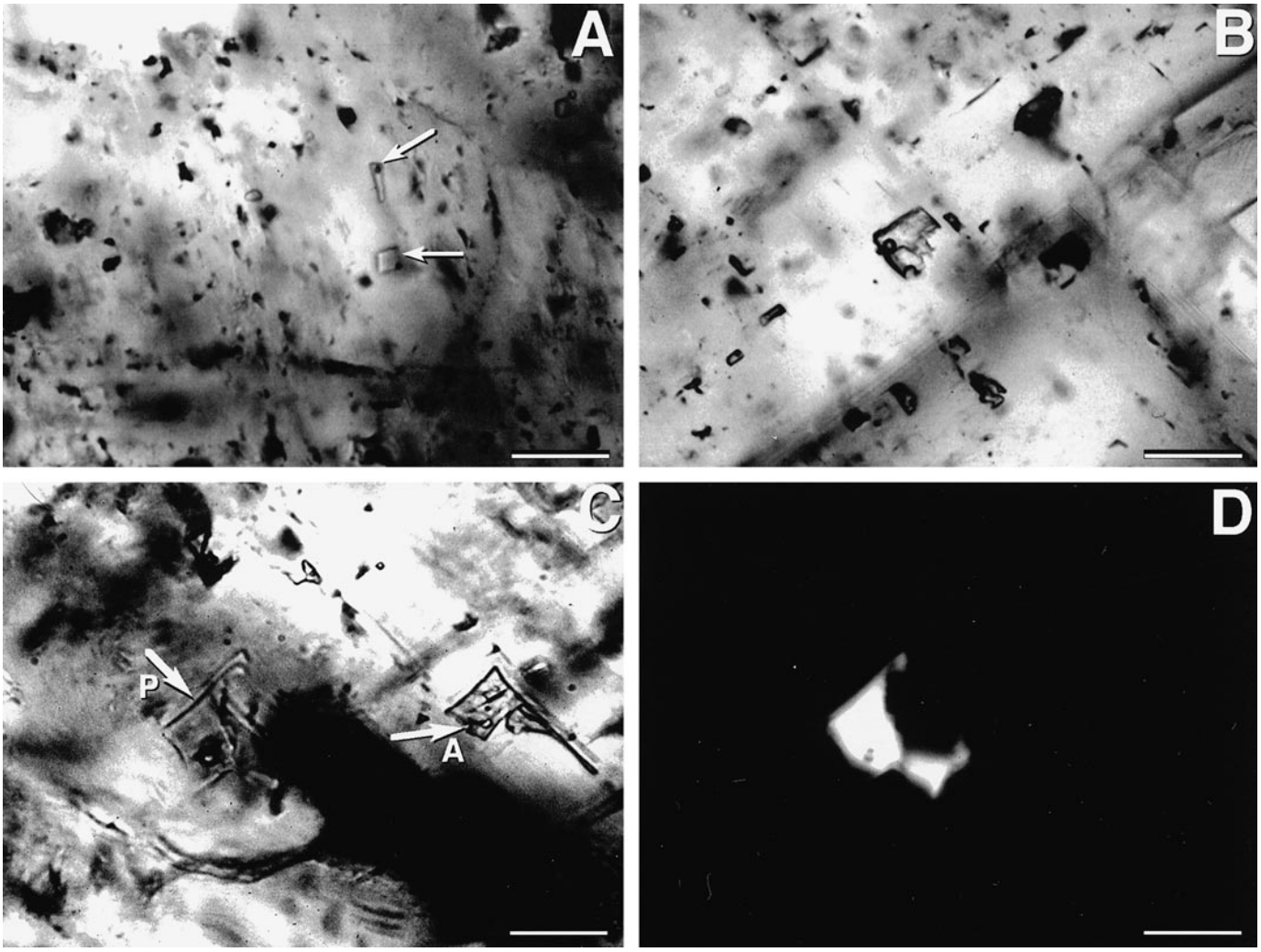

FIG. 8.—Photomicrographs of fluid inclusions. **A)** Fluid inclusions in type 1 cement (arrows) showing tiny vapor bubbles. Scale bar = 50 μm. **B)** Large fluid inclusion (center) and several small inclusions in type 2 saddle dolomite cement showing various sizes ranging from < 4 to 30 μm. Scale bar = 50 μm. **C)** Liquid petroleum inclusion (arrow P) in saddle dolomite cement and aqueous inclusion (arrow A). In plane-polarized light the petroleum inclusion has a light brown color and the aqueous inclusion is colorless. Scale bar = 50 μm. **D)** Same field as in Part C, using epifluorescence. The petroleum inclusion displays bright greenish-yellow fluorescence (visible here as bright area in dark field) under ultraviolet light. Scale bar = 50 μm.

Type 1 cement has a complex CL growth stratigraphy (Fig. 5B) that is roughly correlative throughout the entire Kankakee Arch area. The thickness of individual CL bands decrease downward in each stratigraphic section and to the southeast along the axis of arch, suggesting a descending southward-moving diagenetic fluid (Fig. 10B). Such a movement of diagenetic fluids is also supported by the volume of cement in open space, which decreases in the same directions.

Late Diagenesis

Type 2 (saddle) dolomite cement was precipitated in dissolution-enlarged vugs and fractures during later diagenesis. Saddle dolomite is reported largely along preexisting linear fault zones in the Michigan Basin and in surrounding areas associated with ''fracture-related'' replacement dolomite, which form hydrocarbon reservoirs (Taylor and Sibley 1986; Haefner et al. 1988; Prouty 1989; Granath 1991; Budai and Wilson 1991; Coniglio et al. 1994).

Saddle dolomite in the Kankakee Arch area has petrographic characteristics similar to those of other areas. Core sections (250 and 833, Fig. 1) near the Michigan Basin, which were partially dolomitized in the upper part of the Trenton Limestone, contain abundant saddle dolomite cement in open spaces. The remaining porosity is filled largely by anhydrite and/or gypsum cement, following saddle dolomite precipitation. Farther away from the Michigan Basin, cores where it was observed (447 and 504, Fig. 1) contain only a small amount of saddle dolomite cement.

The number of alternating dull-CL and non-CL zones in type 2 cements also diminishes away from the Michigan Basin. Similar relationships occur in the homogenization temperatures and salinities of fluid inclusions in saddle dolomite cement (Fig. 9), suggesting that the diagenetic fluid emerging from the Michigan Basin cooled and became more dilute during travel toward the Kankakee Arch area (Fig. 9). The presence of hydrocarbon fluid inclusions in saddle dolomite indicates that the flow of late diagenetic fluids to the Kankakee Arch area is closely related with hydrocarbon generation and migration.

High salinities of fluid inclusions and extensive precipitation of evaporite cement following precipitation of saddle dolomite indicate that the dolomitizing fluid generated from the Michigan Basin was saline, possibly resulting from dissolution of evaporites. The less radiogenic strontium-isotope value in saddle dolomite compared to other dolomite types suggests that this diagenetic fluid was not associated with shale or crystalline basement, and indirectly supports an evaporite dissolution origin. Lower $\delta^{18}O$ values and higher fluid-inclusion homogenization temperatures indicate that the late diagenetic fluid was generated during deeper burial in the basin.

In a study of the Wyandot fracture zone in northwest Ohio, Haefner et al. (1988) suggested that fracture-related dolomite was deposited by warm, moderately saline, Mg- and Fe-bearing brines provided from adjacent sedimentary basins. On the basis of regional variation of stable-isotope compositions of dolomite in the Michigan Basin and its close association with MVT mineralization and hydrocarbon migration, they suggested that an ascending basinal brine mixing with meteoric water recharged from the basin margin was responsible for formation of fracture-related dolomite

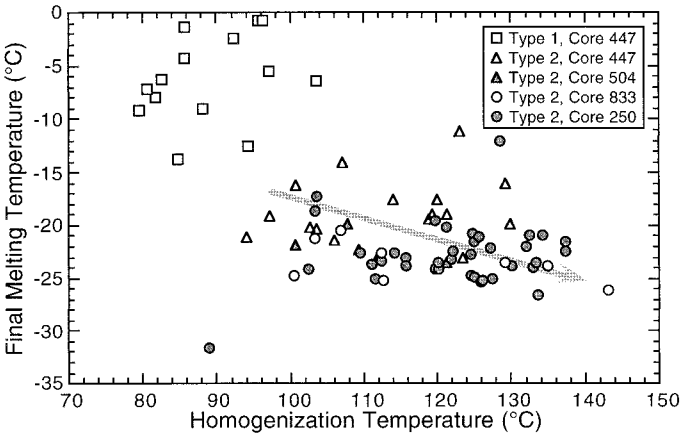

FIG. 9.—Last ice-melting and homogenization temperatures for primary fluid inclusions in dolomite cement. Calculated salinities for the system H_2O–NaCl are shown (Potter et al. 1978). However, fluids likely are complex Na–Ca–MgCl brines. Fluid-inclusion homogenization temperatures and salinities in type 2 saddle dolomite cement display a statistical decrease in temperature and increase in salinity (arrow) from near the axis of the Kankakee Arch (cores 447 and 504) to the margin of the Michigan Basin (cores 833 and 250).

(Budai and Wilson 1991). Granath (1991) suggested that saddle dolomite cement in the Albion–Scipio Trend of the Michigan Basin was precipitated from a hot brine during deep burial of the Trenton Limestone, on the basis of its lower $\delta^{18}O$ values and higher homogenization temperatures of fluid inclusions. She also observed that $^{87}Sr/^{86}Sr$ ratios of saddle dolomites overlapped with the range of Late Silurian seawater, and invoked a Late Silurian seawater influence in the dolomitizing fluid (Granath 1991). Coniglio et al. (1994) suggested that fracture-related dolomites were formed by fluids generated through compaction flow of the central parts of the basin, reflux from the overlying Silurian strata, or invasion of younger fluids. High homogenization temperatures of fluid inclusions, which could not be explained by a deep-burial origin, were thought to have been caused by rising hydrothermal fluids (Coniglio et al. 1994). Our data are consistent with these earlier studies, in indicating that late diagenetic fluids were generated within the Michigan Basin during deep burial. The fluids likely emerged along fractures and faults and were driven by compaction of sedimentary rocks in the Michigan Basin.

CONCLUSIONS

The Trenton and Black River Limestones are extensively dolomitized along the axis of the Kankakee Arch, with the amount of dolomite decreasing to the south and southeast. Three stages of dolomitization, involving different fluids, are identified on the basis of petrographic and geochemical characteristics of the dolomites. On the basis of petrography and isotope geochemistry, nonferroan planar dolomite is interpreted to have formed by evolved Middle and Late Ordovician seawater during the deposition of the overlying Maquoketa Shale. Geochemical and petrographic evidence indicates that during compaction of the overlying shale the early-formed nonferroan planar dolomite neomorphosed to ferroan nonplanar and planar dolomite in the upper part of the Trenton Limestone. At this time type 1 dolomite cement was precipitated into open spaces by the same or similar shale-derived fluids. Distribution of ferroan dolomite is confined to areas where planar dolomite previously existed adjacent to the overlying shale. This indicates that the fluids expelled from overlying shale did not contain enough Mg^{2+} to dolomitize limestone. Type 2 saddle dolomite cements precipitated late in the diagenetic process from higher-temperature, saline fluids emerging from the Michigan Basin, as indicated by fluid inclusions and isotope geochemistry.

ACKNOWLEDGMENTS

Funding for this project was provided by the Korean Research Foundation and University of Missouri Research Board. We thank the Doe Run Company, Viburnum, Missouri, for access to numerous drill core logs covering northern Indiana. Mrs. Sherry Cazee of the Indiana Geological Survey was very helpful in identifying and sampling drill core used in this study. We thank Drs. Gordon S. Fraser and Brian D. Keith, also with the Indiana Geological Survey, for very useful discussions concerning this study. Strontium isotope analyses were performed at the University

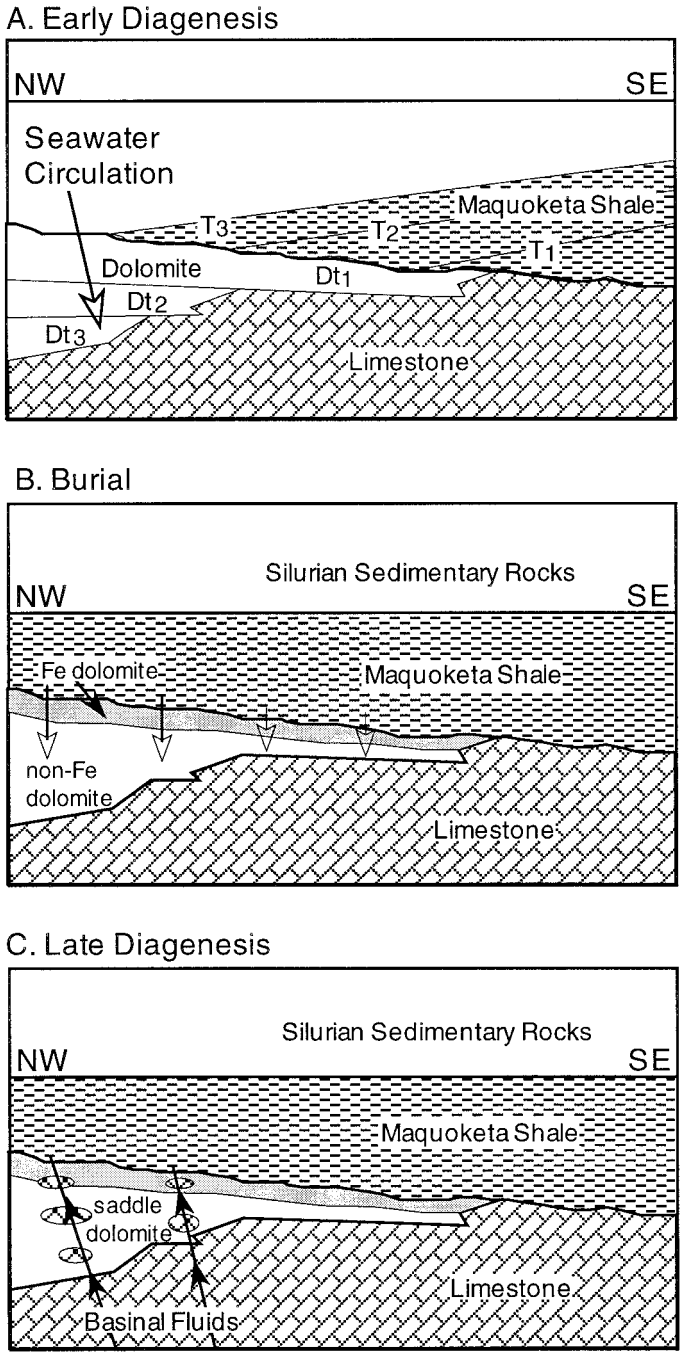

FIG. 10.—Diagrams showing inferred stages of dolomitization in the Trenton and Black River Limestones. **A)** Early Diagenesis—during deposition of the overlying Maquoketa Shale, the Trenton and Black River Limestones were dolomitized by influx of seawater. Dt_n represents the dolomite body formed at time T_n. Seawater did not move into limestone underlying the advancing shale. This resulted in a wedge-shaped dolomite body tapering upward toward the south and southeast. **B)** Burial—in the upper part of the Trenton Limestone, early-formed nonferroan planar dolomite neomorphosed to ferroan nonplanar and planar dolomite by reaction with fluids expelled from the overlying shale during burial. Type 1 dolomite cement precipitated into open spaces from the same or similar fluid. **C)** Late Diagenesis—Type 2 saddle dolomite precipitated in open space from saline, basinal brines emerging from the Michigan Basin along fractures and faults.

of Texas, Dallas and Dr. Scott J. Carpenter, University of Texas at Dallas, provided expertise on strontium isotope analysis. We also thank Dong-Ho Lee, University of Texas at Dallas, for help with strontium-isotope analysis. Francis C. Furman is thanked for his interest and fruitful discussion. We also thank Paul E. Gerdemann, Vice President of Exploration (Ret.), St. Joe Minerals Corporation, for originally suggesting this project. This paper greatly profited by reviews of Eric Mountjoy, S.J. Mazzullo, and one anonymous reviewer.

REFERENCES

Badiozamani, K., 1973, The Dorag dolomitization model—Application to the Middle Ordovician of Wisconsin: Journal of Sedimentary Petrology, v. 43, p. 965–984.

Boles, J.R., and Franks, S.G., 1979, Clay diagenesis in Wilcox Sandstones of southwest Texas: implications of smectite diagenesis on sandstone cementation: Journal of Sedimentary Petrology, v. 49, p. 55–70.

Budai, J.M., and Wilson, J.L., 1991, Diagenetic history of the Trenton and Black River Formations in the Michigan Basin, *in* Catacosinos, P.A., and Daniels, P.A. Jr., eds., Early Sedimentary Evolution of the Michigan Basin: Geological Society of America, Special Paper 256, p. 73–88.

Burke, W.H., Denison, R.E., Hetherington, E.A., Koepnick, R.B., Nelson, H.F., and Otto, J.B., 1982, Variation of seawater $^{87}Sr/^{86}Sr$ throughout Phanerozoic time: Geology, v. 10, p. 516–519.

Collinson, C., Sargent, M.L., and Jennings, J.R., 1988, Illinois Basin region, *in* Sloss, L.L., ed., Sedimentary Cover—North American Craton, U.S.: Geological Society of America, The Geology of North America, vol. D-2, p. 383–426.

Coniglio, M., Sherlock, R., Williams-Jones, A.E., Middleton, K., and Frape, S.K., 1994, Burial and hydrothermal diagenesis of Ordovician carbonates from the Michigan Basin, Ontario, Canada, *in* Purser, B.H., Tucker, M.E., and Zenger, D.H., eds., Dolomites: A Volume in Honour of Dolomieu: International Association of Sedimentologists, Special Publication 21, p. 231–254.

Cook, T.D., and Bally, A.W., eds., 1975, Stratigraphic Atlas of North and Central America: Princeton, New Jersey, Princeton University Press, 272 p.

Crawford, M.L., 1981, Phase equilibria in aqueous fluid inclusions, *in* Hollister, L.S., and Crawford, M.L., eds., Fluid inclusions: Applications to Petrology: Mineralogical Association of Canada, Short Course, p. 75–100.

Curtis, C.D., 1967, Diagenetic iron minerals in some British Carboniferous sediments: Geochimica et Cosmochimica Acta, v. 31, p. 2109–2123.

DeHaas, R.J., and Jones, M.W., 1989, Cave-levels of the Trenton–Black River Formations in central southern Michigan, *in* Keith, B.D., ed., The Trenton Group (Upper Ordovician Series) of Eastern North America: American Association of Petroleum Geologists, Studies in Geology 29, p. 237–266.

Dickson, J.A.D., 1966, Carbonate identification and genesis as revealed by staining: Journal of Sedimentary Petrology, v. 36, p. 491–505.

Fara, D.R., and Keith, B.D., 1989, Depositional facies and diagenetic history of the Trenton Limestone in northern Indiana, *in* Keith, B.D., ed., The Trenton Group (Upper Ordovician Series) of eastern North America: American Association of Petroleum Geologists, Studies in Geology, v. 29, p. 277–298.

Fisher, J.H., Barratt, M.W., Droste, J.B., and Shaver, R.H., 1988, Michigan Basin, *in* Sloss, L.L., ed., Sedimentary cover—North American craton, U.S.: Geological Society of America, The Geology of North America, vol. D-2, p. 361–381.

Friedman, I., and O'Neil, J.R., 1977, Compilation of stable isotope fractionation factors of geochemical interest: U. S. Geological Survey, Professional Paper 440-KK, 12 p.

Granath, V.C., 1991, Geochemical constraints on the origin of dolomite in the Ordovician Trenton and Black River Limestones, Albion–Scipio area, Michigan (abstract): American Association of Petroleum Geologists, Bulletin, v. 75, p. 584–585.

Gregg, J.M., and Sibley, D.F., 1984, Epigenetic dolomitization and the origin of xenotopic dolomite texture: Journal of Sedimentary Petrology, v. 54, p. 908–931.

Guthrie, J.M., and Pratt, L.M., 1994, Geochemical indicators of depositional environment and source-rock potential for the Upper Ordovician Maquoketa Group, Illinois Basin: American Association of Petroleum Geologists, Bulletin, v. 78, p. 744–757.

Haefner, R.J., Mancuso, J.J., Frizado, J.P., Shelton, K.L., and Gregg, J.M., 1988, Crystallization temperatures and stable isotope compositions of Mississippi Valley–type carbonates and sulfides of the Trenton Limestone, Wyandot County, Ohio: Economic Geology, v. 83, p. 1061–1069.

Hurley, N.F., and Budros, R., 1990, Albion–Scipio and Stoney Point Fields—U.S.A. Michigan Basin, *in* Beaumont, E.A., and Foster, N.H., eds., Stratigraphic Traps I: American Association of Petroleum Geologists, Treatise of Petroleum Geology, Atlas of Oil and Gas Fields, p. 1–37.

Hurley, N.F., and Swager, N.R., 1991, A classic-fracture-controlled dolomite reservoir: Albion–Scipio Trend, Michigan (abstract): American Association of Petroleum Geologists, Bulletin, v. 75, p. 1806.

Irwin, H., 1980, Early diagenetic precipitation and pore fluid migration in the Kimmeridge clay of Dorset, England: Sedimentology, v. 27, p. 577–591.

Keith, B.D., 1985, Facies, diagenesis, and the upper contact of the Trenton Limestone of northern Indiana, *in* Cercone, C.R., and Budai, J.M., eds., Ordovician and Silurian Rocks of the Michigan Basin and its margins: Michigan Basin Geological Society, Special Paper 4, p. 15–32.

Keith, B.D., 1989, Regional facies of Upper Ordovician Series of eastern North America, *in* Keith, B.D., ed., The Trenton Group (Upper Ordovician Series) of Eastern North America: American Association of Petroleum Geologists, Studies in Geology 29, p. 1–16.

Keith, B.D., and Wickstrom, L.H., 1993, Trenton Limestone—The karst that wasn't there or was it?, *in* Fritz, R.D., Wilson, J.L., and Yurewicz, D.A., eds., Paleokarst Related Hydrocarbon Reservoirs: SEPM, Core Workshop 18, p. 167–179.

Kolata, D.R., and Graese, A.M., 1983, Lithostratigraphy and depositional environments of the Maquoketa Group (Ordovician) in northern Illinois: Illinois State Geological Survey, Circular 537, 30 p.

Kolata, D.R., and Nelson, W.J., 1990, Tectonic history of the Illinois Basin, *in* Leighton, M.W., Kolata, D.R., Oltz, D.F., and Eidel, J.J., eds., Interior Cratonic Basins: American Association of Petroleum Geologists, Memoir 51, p. 263–286.

Land, L.S., 1985, The origin of massive dolomite: Journal of Geological Education, v. 33, p. 112–125.

Land, L.S., 1991, Dolomitization of the Hope Gate Formation (north Jamaica) by seawater: reassessment of mixing-zone dolomite, *in* Taylor, H.P., Jr., O'Neil, J.R., and Kaplan, I.R., eds., Stable Isotope Chemistry: A Tribute to Samuel Epstein: Geochemical Society, Special Publication 3, 121–133.

Lohmann, K.C., 1988, Geochemical patterns of meteoric diagenetic systems and their application of studies of paleokarst, *in* James, N.P., and Choquette, P.W., eds., Paleokarst: New York, Springer-Verlag, p. 58–80.

Lohmann, K.C., and Walker, J.C.G., 1989, The $\delta^{18}O$ record of Phanerozoic abiotic marine calcite cements: Geophysical Research Letters, v. 16, p. 319–322.

McCrea, J.M., 1950, The isotope chemistry of carbonates and a paleotemperature scale: Journal of Chemical Physics, v. 18, p. 849–857.

McHargue, T.R., and Price, R.C., 1982, Dolomite from clay in argillaceous or shale-associated marine carbonates: Journal of Sedimentary Petrology, v. 52, p. 873–886.

Potter, R.W., II, Clynne, M.A., and Brown, D.L., 1978, Freezing point depression of aqueous sodium chloride solutions: Geology, v. 73, p. 284–285.

Prouty, C.E., 1989, Trenton exploration and wrench tectonics: Michigan Basin and environs, *in* Keith, B.D., ed., The Trenton Group (Upper Ordovician Series) of Eastern North America: American Association of Petroleum Geologists, Studies in Geology 29, p. 207–236.

Rooney, L.F., 1966, Evidence of unconformity in the Trenton Limestone in Indiana and adjacent states: American Association of Petroleum Geologists, Bulletin, v. 50, p. 533–546.

Sibley, D.F., and Gregg, J.M., 1987, Classification of dolomite rock textures: Journal of Sedimentary Petrology, v. 57, p. 967–975.

Stueber, A.M., Pushkar, P., and Hetherington, E.A., 1987, A strontium isotopic study of formation waters from the Illinois basin, U.S.A.: Applied Geochemistry, v. 2, p. 477–494.

Taylor, T.R., and Sibley, D.F., 1986, Ferroan dolomite in the Trenton Formation, Ordovician Michigan Basin: Sedimentology, v. 33, p. 61–86.

Received 24 August 1998; accepted 18 April 1999.